Photoproduction of Neutral ρ Mesons*†

L. J. LANZEROTTI,‡ R. B. BLUMENTHAL,§ D. C. EHN, W. L. FAISSLER,‖ P. M. JOSEPH,**
F. M. PIPKIN, J. K. RANDOLPH, J. J. RUSSELL, D. G. STAIRS,†† AND J. TENENBAUM
Cyclotron Laboratory, Harvard University, Cambridge, Massachusetts

(Received 8 August 1967)

An experimental study of the photoproduction of charged pion pairs is reported. The pions were detected with two mirror-image magnetic spectrometers, each of which consisted of a half-quadrupole magnet and a number of scintillation counters. The dipion mass spectrum was searched over by fixing the position of the spectrometer arms, fixing the maximum photon energy, and varying the current in each of the half-quadrupole magnets. Measurements were made for symmetrical pairs with opening angles of 18.2° and 32.1° for photon energies of 5.5 and 3.0 BeV and for hydrogen and carbon targets; some measurements were also made with aluminum and copper targets. Measurements were made of asymmetric pairs and symmetrical pairs whose resultant momentum made an angle of 6° with respect to the photon beam. In the course of the experiment, the invariant mass of the dipion system ranged from 0.300 to 1.50 BeV. The only significant structure seen was at the mass of the ρ^0 meson. The measurements showed that the ρ photoproduction from hydrogen is due to a diffractionlike mechanism. The data from complex nuclei showed that the production at 0° was coherent and that the ρ's were completely polarized. No evidence was found for a forward-backward asymmetry in the decay of the photoproduced ρ's.

I. INTRODUCTION

DURING recent years a number of unstable multipion resonant states have been discovered.[1] Attempts to observe their photoproduction with incoming γ-ray energies under 2 BeV have been hampered by the small amount of energy available. At such energies it is difficult to separate nonresonant multiplets of pions from resonant states. It is also difficult to achieve a sufficient variation of bombarding energy to discern significant dynamic properties of the production processes.[2]

With γ-ray energies up to 6 BeV now available at the Cambridge Electron Accelerator, we have undertaken a survey of $\pi^+\pi^-$ pair production to search for resonant states. The experiment was performed with apparatus designed initially to study e^+e^- pair production,[3] and hence the emphasis was on the production of high-energy pions at small angles with respect to the incoming γ-ray beam.

Estimates of the photoproduction cross sections for vector mesons have been made by Drell and Berman[4] on the basis of several plausible models. Their calculations lead one to expect a large cross section for the photoproduction of neutral ρ mesons.

The experiment reported here was designed to study the two-pion mass spectrum in two experimental configurations. The first, with a small opening angle between the pion pair, allowed observation of the expected ρ^0 meson at a relatively high incoming γ-ray energy (4.4 BeV). The second, with a larger opening angle between the pair, covered a much wider range of resonant masses and detected ρ^0 mesons at a lower γ-ray energy (2.5 BeV). In the second arrangement, two mass searches were performed: one to detect dipion states produced along the γ-ray direction, the other to detect dipion states sufficiently different in direction from that of the γ ray to reduce the suppression at 0^0 by polarization effects.

II. APPARATUS

Figures 1 and 2 show the layout of the experiment. Modifications were made to the system used previously to measure electron-pair production[3] in order to achieve larger angles between the beam and outgoing particle directions and to improve the momentum and angular resolution.

A bremsstrahlung beam produced inside the synchrotron when the internal electron beam struck a $\frac{1}{10}$ radiation length tungsten ribbon was collimated to a spot $\frac{1}{4}$ in. high by $\frac{1}{2}$ in. wide at the target position. The spill length varied from 1.3 to 1.5 msec. The duty cycle of the beam was continuously monitored and had an average value of 5%. The total energy of the beam was measured by a Wilson-type quantameter downstream from the spectrometers.[5]

* Research supported by the U. S. Atomic Energy Commission under Contract No. AT(30-1)-2752.

† This paper is based in part on a thesis submitted by one of the authors (L.J.L.) to Harvard University in partial fulfillment of the requirements for the PhD. degree.

‡ Present Address: Bell Telephone Laboratories, Murray Hill, N. J.

§ Present address: Physics Department, University of Pennsylvania, Philadelphia, Pa.

‖ Present address: Physics Department, Northeastern University, Boston, Mass.

** Present address: Physics Department, Cornell University, Ithaca, N. Y.

†† Present address: Physics Department, McGill University, Montreal, Canada.

[1] A. H. Rosenfeld, A. Barbaro-Galtieri, W. J. Podolsky, L. R. Price, P. Soding, C. G. Wohl, M. Ross, and W. J. Willis, Rev. Mod. Phys. 39, 1 (1967).

[2] D. McLeod, S. Richert, and A. Silverman, Phys. Rev. Letters 7, 383 (1961); A. D. Franklin, D. R. Rust, A. Silverman, C. K. Sinclair, and R. M. Talman, *ibid.* 13, 491 (1964); R. Del Fabbro, M. De Prentis, R. Jones, G. Marini, A. Odian, G. Stoppini, and L. Tau, *ibid.* 12, 674 (1964).

[3] R. B. Blumenthal, D. C. Ehn, W. L. Faissler, P. M. Joseph, L. J. Lanzerotti, F. M. Pipkin, and D. G. Stairs, Phys. Rev. 144, 1199 (1966).

[4] S. M. Berman and S. D. Drell, Phys. Rev. 133, B791 (1964).

[5] R. R. Wilson, Nucl. Instr. Methods 1, 101 (1957).

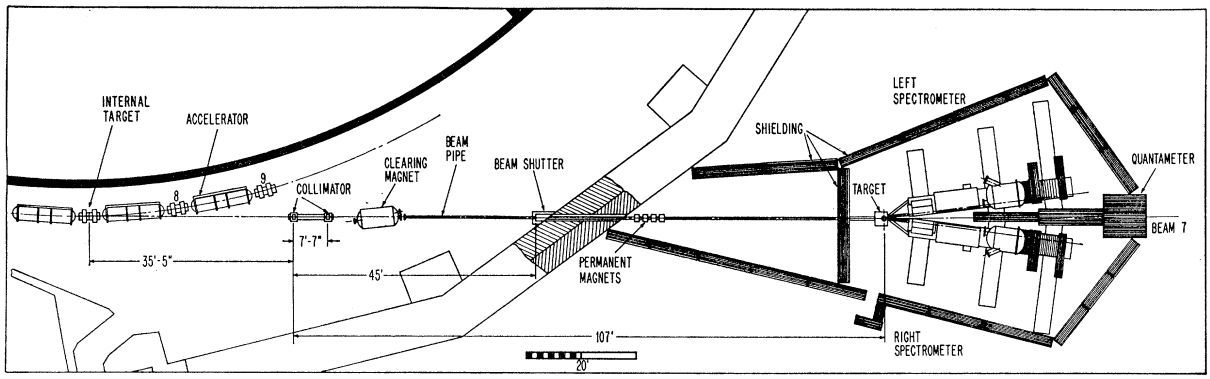

FIG. 1. A diagram showing the γ-ray beam and the location of the spectrometers with respect to the accelerator.

Solid targets of various thickness or a $2\frac{1}{2}$-in.-long liquid-hydrogen target could be placed at the pivot point of the spectrometer arms. The carbon targets were 1 or 2 in. thick, the aluminum target was $\frac{1}{2}$ in. thick, and the copper target was $\frac{1}{8}$ in. thick.

Each spectrometer arm consisted of $\frac{1}{2}$ of a conventional 12-in.-aperture, 48-in.-long quadrupole magnet and an array of scintillation counters. Each half-quadrupole was provided with an iron image plate; this made it possible to maintain a normal quadrupole field in the magnet aperture and to allow the spectrometers a much closer approach to the γ-ray beam. The two spectrometers were calibrated to an accuracy of 1% by magnetic field and floating wire measurements.

Figure 3 shows schematically the array of counters used to define the particle trajectories. A particle on one arm was defined by a fourfold coincidence between scintillation counters S_1, S_2, S_3, and S_4. With the lead obstacle placed in its center, the vertically focusing half-quadrupole magnet allowed only particles in a small momentum range to cross the axis of the system between counters S_2 and S_3. Counter S_1, $2\frac{1}{2}$ in. high and $7\frac{1}{2}$ in. wide, defined the solid angle of the spectrometer. The spacing of S_2 and S_3 set the momentum acceptance. For a γ-ray beam $\frac{1}{4}$ in. high and $\frac{1}{2}$ in. wide at the pivot, the angular acceptance in the horizontal plane was ± 0.7 deg, the momentum acceptance was 8% full width at half-maximum, and the phase-space acceptance $\Delta\Omega\Delta p/p$ was 0.052 msr. Scintillation counter S_4 accepted all the particles from the target which passed through S_1, S_2, and S_3 and served only to reduce the background. Counters A1–A7 and M1–M5 subdivided the angular and momentum acceptance of the system. Each angle counter provided a fine angular resolution of $\pm 0.1°$ and the separation of the individual momentum counters provided a fine momentum resolution of $\pm 1\%$.

The counters were arranged to distinguish between trajectories passing above and below the obstacle; thus there were two identical channels on each arm. The four channels will be denoted LU, LD, RU, and RD where L=left, R=right, U(D) denotes the trajectory emerging from the lower (upper) half of the quadrupole.

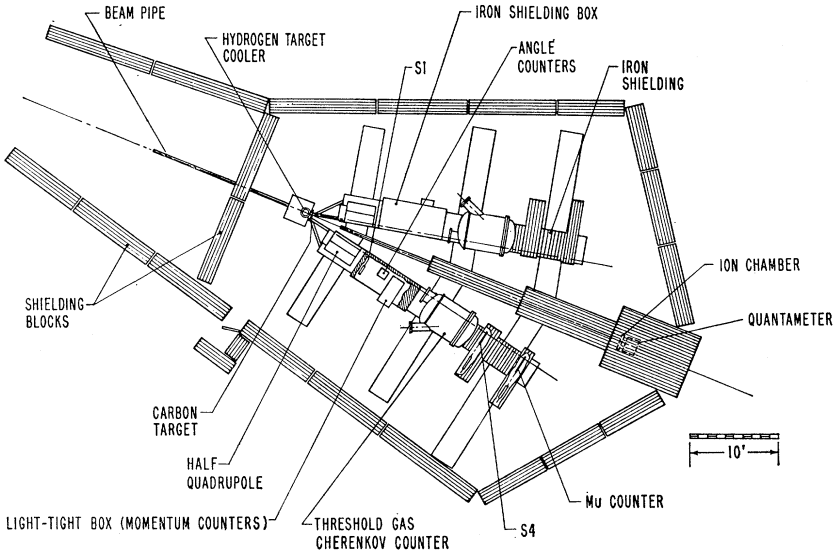

FIG. 2. A diagram showing the target, the spectrometer arms, and the quantameter.

No positive particle identification was made of the majority of the pairs observed. A threshold Čerenkov counter C, which has been described previously,[3] was used to identify electrons. A scintillator Mu counted particles which passed through 3 ft of iron behind the Čerenkov counter. Experimental upper limits to the contamination due to the electron and muon pairs were 0.1 and 0.8%, respectively.

Figure 4 is a simplified diagram of the electronics used in the LD-RU channel. Except for the discriminators, which were commercially built Chronetics discriminators, the circuits were designed and engineered by several members of the experimental group. The coincidence circuits were operated with a 13-nsec resolving time. In addition to the primary coincidence LU-RD, single-channel rates including the Čerenkov counter C and range counter Mu, pair rates such as LDC–RUC, LDMu–RUMu, and various random coincidences were formed and monitored continuously.

A set of 20-nsec bit gates, also locally designed, were used to interrogate the counters A1–A7, M1–M5, the Čerenkov and range counters whenever an event satisfying a trigger requirement occurred. The trigger requirement was normally that any one of the coincidences LU-RD, LD-RU, LU-RU, or LD-RD had occurred. The information in the bit gates was then transferred by standard, commercially available computer logic to a PDP-1 computer which recorded the data on magnetic tape and performed a preliminary analysis. No significant additional structure in the mass spectra was observed by using the improved mass resolution afforded by these counters. The final analysis of the data reported here is based entirely on the data obtained from the trigger counters S_1–S_4.

III. DATA-TAKING PROCEDURE

Most of the data were taken with the two spectrometer arms placed at equal angles with respect to the incoming γ-ray beam and set to accept particles of opposite charge and equal momentum. In this configuration, the pairs LU-RD and LD-RU are due to two particles whose resultant momentum makes an angle of 0° with the γ-ray beam. The pairs LU-RU and LD-RD have a resultant momentum which is in the vertical plane containing the γ-ray beam and which makes an angle of 3.5° with respect to the horizontal plane. The 3.5° angle is due to the distance of the entrance apertures of the quadrupole spectrometers from the horizontal plane. For a given placement of the spectrometer arms, the opening angle for the LU-RU and LD-RD pairs is slightly smaller than that for the LU-RD and LD-RU pairs.

To obtain data on the production of pairs with resultant momenta at larger angles, the spectrometer arms were placed asymmetrically with their bisector at 6° relative to the γ-ray beam and set to accept equal momenta. By setting both the angles and the momenta

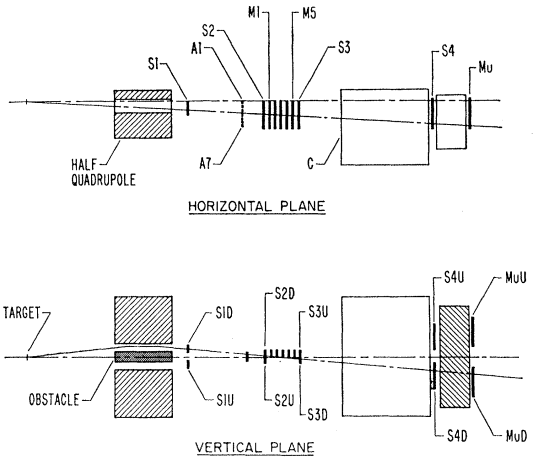

FIG. 3. Schematic drawing of one of the two spectrometer arms showing the counters used to define a particle and measure its momentum.

of the arms with appropriate asymmetry, pairs which share the available energy unequally but still have a resultant momentum along the direction of the γ-ray beam were studied.

With the peak energy of the bremsstrahlung spectrum fixed, for each angular configuration the momentum distribution of pair events was measured. For most of the runs, the peak bremsstrahlung energy was 5.5 BeV and the momentum of each of the observed particles was varied from 0.5 to 2.65 BeV/c. Such distributions were obtained with the bisector of the arms at 0^0 with respect to the γ-ray beam and with the opening angle for the LU-RD and LD-RU pairs 18.2° and 32.1°. With the bisector of the arms at 6°, only data for a pion opening angle of 32.1° could be obtained.

To keep random-coincidence corrections small, the most important class of random coincidences, that

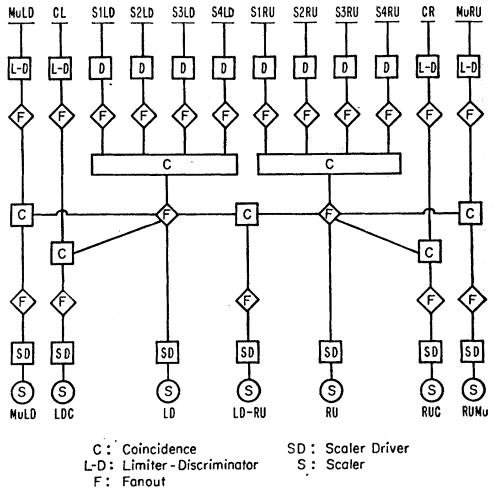

FIG. 4. Simplified block diagram of the electronics used for the LD-RU pairs. Not shown are the other circuits used to monitor the randoms.

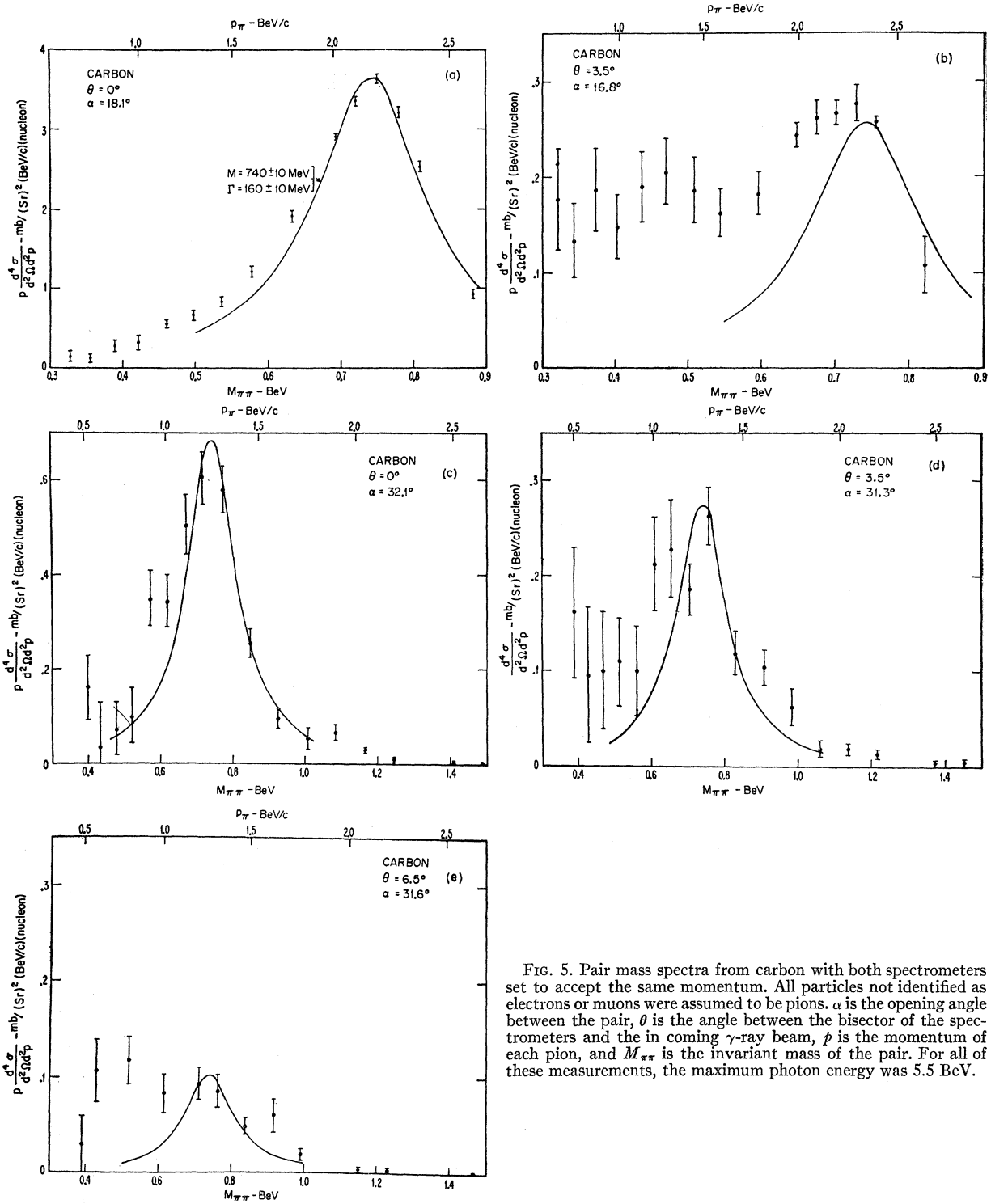

FIG. 5. Pair mass spectra from carbon with both spectrometers set to accept the same momentum. All particles not identified as electrons or muons were assumed to be pions. α is the opening angle between the pair, θ is the angle between the bisector of the spectrometers and the in coming γ-ray beam, p is the momentum of each pion, and $M_{\pi\pi}$ is the invariant mass of the pair. For all of these measurements, the maximum photon energy was 5.5 BeV.

between two real but uncorrelated particles, one on each arm, was monitored continuously. This random rate was never allowed to exceed 10% of the real pair rate. The counting rate in the counters showing the largest background rates was monitored continuously, and the beam intensity and target thickness were varied so as to keep the dead-time loss due to all the counters less than 10%.

Target-out rates were less than 5% except when the hydrogen target was in place and the spectrometer arms

were set at the smallest angle. Under these circumstances, the target-out rate due to a stainless-steel vacuum window upstream of the hydrogen target was 50%.

Complete spectra were obtained with both hydrogen and carbon. The results of different runs were corrected for dead-time losses and target out before they were combined. A 17% correction was applied to the carbon data to correct for absorption of the incoming γ-ray beam and the outgoing pions.[6] These spectra, reduced to $pd^4\sigma/d\Omega^2dp^2$, the pair-production cross-section differential in the solid angle and momentum of each of the pions multiplied by the momentum of one of the pions and normalized to one equivalent incoming quantum and to one target nucleon, are shown in Figs. 5 and 6. An analysis to be described later shows that when the spectra are plotted in this way, a two-pion resonance will appear as an undistorted Breit-Wigner (BW) curve.

IV. ANALYSIS OF DATA

We can use the expression

$$M^2=(p_1+p_2)^2=(E_1+E_2)^2-(\mathbf{p}_1+\mathbf{p}_2)^2 \quad (1)$$

to calculate from the measured direction and momentum of each member of an observed pair the magnitude of the invariant 4-momentum of the pair. This gives the mass of the pair or its equivalent the total energy of the pair in its c.m. system. If we assume that both members of the pair are pions, we can write

$$M_{2\pi}^2=2m_\pi^2+2E_1E_2(1-\beta_1\beta_2\cos\alpha). \quad (2)$$

Here β is the velocity of the pion and α is the angle between the pions. For symmetric pairs and energies such that $E^2\gg m_\pi^2$, Eq. (2) becomes

$$M_{2\pi}^2=4m_\pi^2+4p^2\sin^2(\tfrac{1}{2}\alpha). \quad (3)$$

The only significant peaks in the spectra shown in Figs. 5 and 6 occur at $M_{2\pi}\approx 750$ MeV, the mass of the well-known neutral ρ meson.

To extract from the spectra a cross section for production of the ρ^0, it is necessary to calculate the detection efficiency of the system for the decay pions from the ρ^0. This requires an integration of the distribution of the pion pairs over the acceptance of the system. This integration can be carried out in terms of any equivalent set of six variables; the most useful sets are those in which the distribution functions are simple in form. We have used θ, φ, k, m, θ^*, and φ^*, where θ, φ are the spherical polar coordinates of the ρ^0 in the laboratory system, k is the energy of the incoming γ ray, m is the mass of the ρ^0, and θ^*, φ^* are the angles in the rest system of the ρ^0 of one of the decay pions relative to the ρ^0 direction.

In terms of these variables the detection efficiency ϵ is given by

$$\epsilon=\frac{1}{4\pi}\int\int\sin\theta d\theta d\varphi\int f(k,k_{\max})\frac{dk}{k}\int F(m,m_0)dm \times\int\int\sin\theta^* d\theta^* d\varphi^* Y(+)Y(-). \quad (4)$$

Here $f(k,k_{\max})/k$ is the bremsstrahlung spectrum and $F(m,m_0)$ is a BW distribution of the form

$$F(m,m_0)=\frac{1}{\pi}\frac{\tfrac{1}{2}\Gamma}{(m-m_0)^2+\tfrac{1}{2}\Gamma^2}. \quad (5)$$

$Y(+)$ and $Y(-)$ are acceptance functions for the spectrometer arms set to accept positive and negative particles, respectively. $Y(\pm)$ is unity if the $\pi^\pm$ is accepted by the system; $Y(\pm)$ is zero if the $\pi^\pm$ fails to pass properly through all the counters. The integral was evaluated by the Monte Carlo technique; a table lookup subroutine generated for the geometry of this experiment was used for $Y(\pm)$. The calculated value of ϵ was later corrected to take account of the deviation from isotropy of the c.m. decay angular distribution. When multiplied by the differential cross section, $d\sigma/d\Omega(\gamma+p\rightarrow p+\rho^0)$, for ρ photoproduction, the detection efficiency ϵ gives the expected counting rate per target particle per equivalent quantum.

It was found that when the calculated values of ϵ were divided by p, the momentum of one of the pions, they reproduced the input BW function with a small increase in width due to the resolution of the spectrometers. An exact analytic expression can be derived for the detection efficiency in the limit of high resolution.[7] This calculation confirms the Monte Carlo calculation and shows that in the high-resolution limit the detection efficiency divided by the momentum of one of the pions reproduces exactly the BW curve which describes the resonance. The increase in width was 14% for the 18.2° opening angle and 4% for the 32.1° opening angle. At the smaller opening angle, for input ρ^0 parameters $m_0=750$ MeV and $\Gamma=140$ MeV, the resulting detection efficiency curve, which is shown in Fig. 7(a), has a width at half-maximum of 160 MeV. At the larger opening angle between the pions, where the mass acceptance of the system is smaller, the calculated efficiency curve, shown in Fig. 7(b) is broadened to only 145 MeV.

From the data in Figs. 5 and 6 it is clear that a BW curve alone will not represent the observed counting rates for low mass values. Such difficulties have been a consistent feature of two-pion mass spectra observed in strong-interaction production experiments and have

[6] Pion-nucleus absorption cross sections were taken from M. J. Longo and B. J. Moyer, Phys. Rev. 125, 701 (1962); Phys. Rev. Letters 9, 466 (1962). The photon absorption probability was taken as 7/9 per radiation length.

[7] L. Litt (private communication).

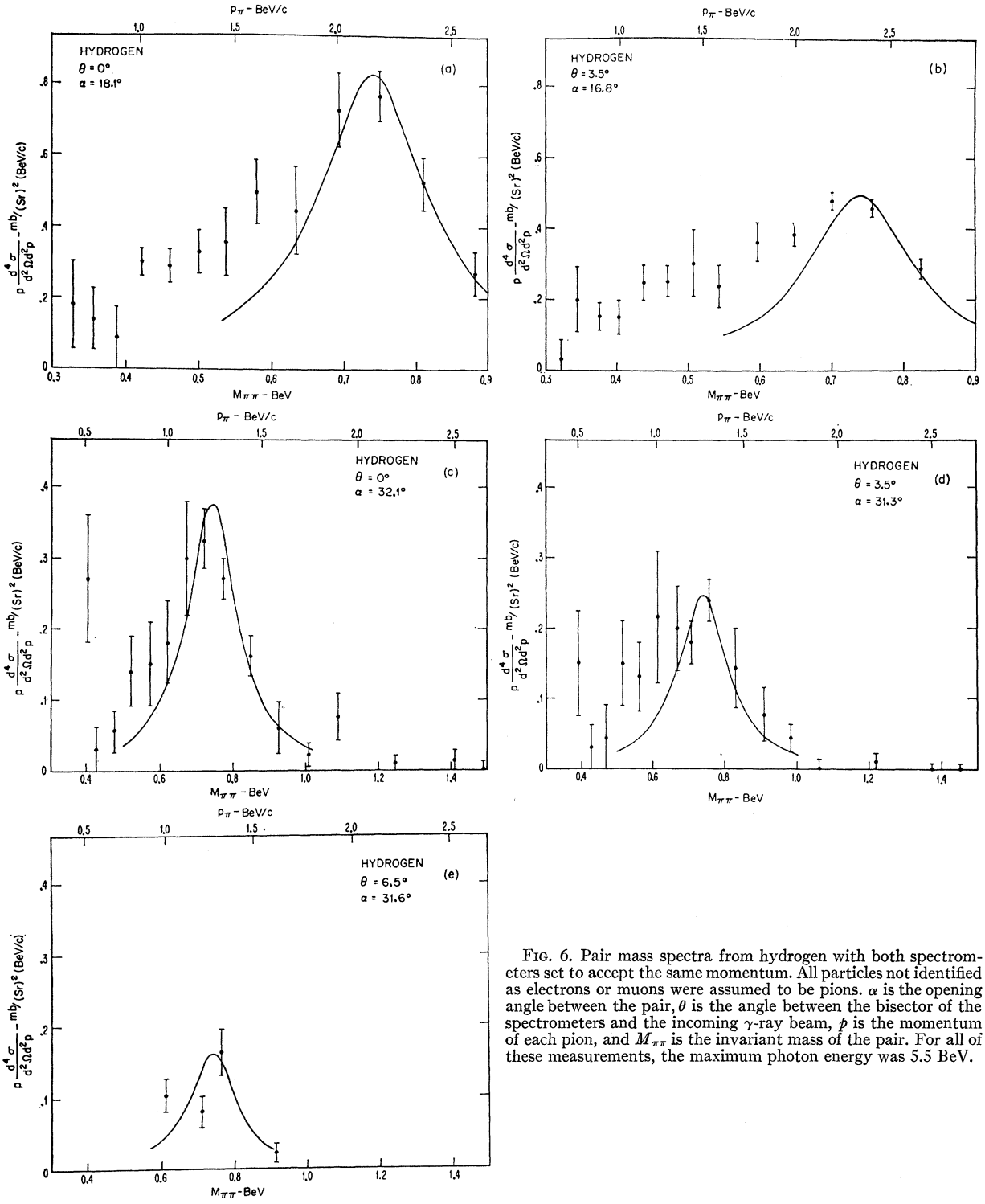

FIG. 6. Pair mass spectra from hydrogen with both spectrometers set to accept the same momentum. All particles not identified as electrons or muons were assumed to be pions. α is the opening angle between the pair, θ is the angle between the bisector of the spectrometers and the incoming γ-ray beam, p is the momentum of each pion, and $M_{\pi\pi}$ is the invariant mass of the pair. For all of these measurements, the maximum photon energy was 5.5 BeV.

given rise to speculation on the existence of a broad resonance at a lower mass than that of the ρ^0.[8] We have estimated the contribution to our spectra at low masses due to two pions from the decay of ω^0 mesons produced

[8] J. B. Kopelman, D. D. Allen, G. Godden, L. Marshall, E. Urvater, R. E. Juhala, and J. I. Rhode, Phys. Letters **22**, 118 (1966). This paper contains references to other experiments involving low-mass dipion enhancements.

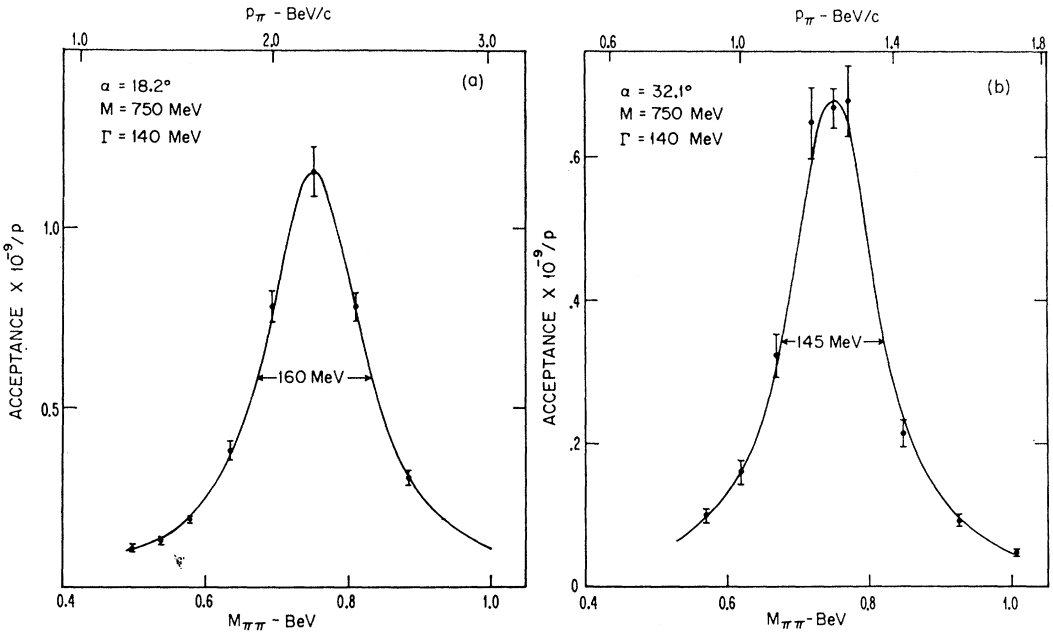

FIG. 7. Calculated efficiency ϵ for detection of ρ^0's in one pair channel of the apparatus. ϵ times $d\sigma/d\Omega$, the laboratory differential cross section for ρ production, gives the counting rate per equivalent quantum per nucleon. α is the opening angle between the detected pions, p_π is the momentum of each pion, and $M_{\pi\pi}$ is the mass of the pair.

by higher-energy photons. From these calculations and the measured total cross sections for ω^0 production,[9] we find a contribution in the 400–650-MeV two-pion mass range which is only $\frac{1}{3}$ of the observed rate. A simple phase-space argument does not explain the excess observed; it predicts a spectrum which is a function only of the momentum of the pions, not of the invariant mass of the pair. It does not predict, for example, the substantial difference between the number of pairs observed with single-pion momenta between 1.5 and 2.0 BeV/c at 18.2° and at 32.1°. The difference is easily understood if a major fraction of these pairs is associated with a state of definite mass.

Since it seems likely that any contributions to the two-pion mass spectra from sources other than the ρ^0 produce a background which is significant only at masses below the central mass of the ρ^0, we have altered the procedure used in a preliminary report on this data.[10] There it was assumed that the non-ρ background was due to phase-space production modified by a matrix element decreasing rapidly with incoming γ-ray energy. This resulted in a sizeable ($\sim$20%) subtraction under the ρ^0 peak at the larger opening angle. We have now instead fitted the experimental points only near and above the peak to a BW curve with the assumption that no background subtraction is required. The rapid drop of the spectra above the ρ^0 peak seems consistent with this treatment.

In contrast to the energy and angle dependence of the pair rate near the ρ^0 peak, the low-mass background seems to occur in all spectra, both in carbon and hydrogen, at nearly the same absolute rate per nucleon. In view of this background, a determination of the resonance parameters is best made from the spectrum having a small percentage of nonresonant background. The carbon spectrum of Fig. 5(a) at $\alpha=18.2°$, $\theta=0°$ was fitted to a curve through the points at $M_{2\pi}\geqslant 700$ MeV and falling $\sim$0.2 mb/sr^2 (BeV/c) below the data for $M_{2\pi}<700$ MeV. The latter requirement is suggested by the nearly constant background at low masses in Fig. 5(b). The resulting best fit gives $M(\rho^0)=740\pm10$ MeV and $\Gamma=160\pm10$ MeV. These parameters were used in the curves fitted to all the other data. The curves shown in Figs. 5(b)–(f) and Fig. 6 were fitted only to the experimental points with $M_{2\pi}$ greater than 700 MeV. The rate at the peak was then read off the fitted curve and assigned an error equal to the error on the individual measurements in the region of the peak.

By using the calculated values of the detection efficiency ϵ corresponding to each set of the experimental variables, the cross sections, $d\sigma/d\Omega(\gamma+p\rightarrow\rho^0+p)$, shown in Table I were obtained. The calculated values of ϵ were doubled to account for the two apertures in each magnet and multiplied by 1.5 on the assumption of complete polarization of the ρ^0 along the direction of the ρ^0 as viewed in the ρ^0 c.m. system.

To check that the rate at the ρ^0 peak was due primarily to the process $\gamma+p\rightarrow\rho^0+p$, the excitation curve data shown in Fig. 8 were taken. The slight difference between the calculated excitation curve and

[9] Brown–Harvard–MIT–Padova–Weizmann Institute Bubble Chamber Group, Phys. Rev. **155**, 1468 (1967).

[10] L. J. Lanzerotti, R. B. Blumenthal, D. C. Ehn, W. L. Faissler, P. M. Joseph, F. M. Pipkin, J. K. Randolph, J. J. Russell, D. G. Stairs, and J. Tenenbaum, Phys. Rev. Letters **15**, 210 (1965).

TABLE I. Differential laboratory cross sections $d\sigma/d\Omega$ for ρ^0 production deduced from the spectra in Figs. 5 and 6. Column 6 gives the estimated correction for inelastic contamination to $d\sigma/d\Omega$. The last two columns give t, the 4-momentum transfer averaged over the acceptance of the apparatus, and $d\sigma/dt$, the differential cross section for elastic ρ^0 photoproduction. Both $d\sigma/d\Omega$ and $d\sigma/dt$ were calculated with the assumption that ρ^0's were completely polarized along the ρ^0 direction as seen in the ρ^0 c.m. system.

Target	θ (deg)	α (deg)	k (BeV)	$d\sigma/d\Omega$ (mb/sr-nucleon)	Inelastic correction	$-t$ ((BeV/c)^2)	$d\sigma/dt$ (elastic) (μb/(BeV/c)^2)
Hydrogen	0.0	18.1	4.40	1.54±0.16	×(0.9±0.1)	0.006	230±30
	3.5	16.8	4.80	0.85±0.09	×(0.9±0.1)	0.090	95±14
	0.0	32.1	2.52	1.12±0.12	×(0.6±0.2)	0.013	350±110
	3.5	31.3	2.60	0.76±0.09	×(0.6±0.2)	0.039	220±74
	6.5	31.6	2.56	0.48±0.12	×(0.6±0.2)	0.096	150±62
Carbon	0.0	18.1	4.40	6.87±0.46	×1.00	0.006	1135±76
	3.5	16.8	4.80	0.43±0.04	×(0.5±0.2)	0.085	29±12
	0.0	32.1	2.52	2.05±0.21	−0.44±0.22	0.013	840±160
	3.5	31.3	2.60	0.85±0.10	−0.32±0.15	0.038	310±88
	6.5	31.6	2.56	0.30±0.06	−0.20±0.10	0.092	52±62

the accurate carbon data in Fig. 8(a) can be understood on the basis of the broadening of the momentum resolution due to target size. With the hydrogen spectra is shown the excitation curve for elastic production together with the inelastic process $\gamma+p\rightarrow\rho^0+N^*$ (1238). The rapid increase in yield between 4.4 and 4.8 BeV seen in Figs. 8(c) and 8(d) excludes inelastic contributions of more than 20%. We have applied to the corresponding 5.5 BeV ρ^0 data a (10±10)% correction for inelastic contamination. For carbon at 3.5°, the

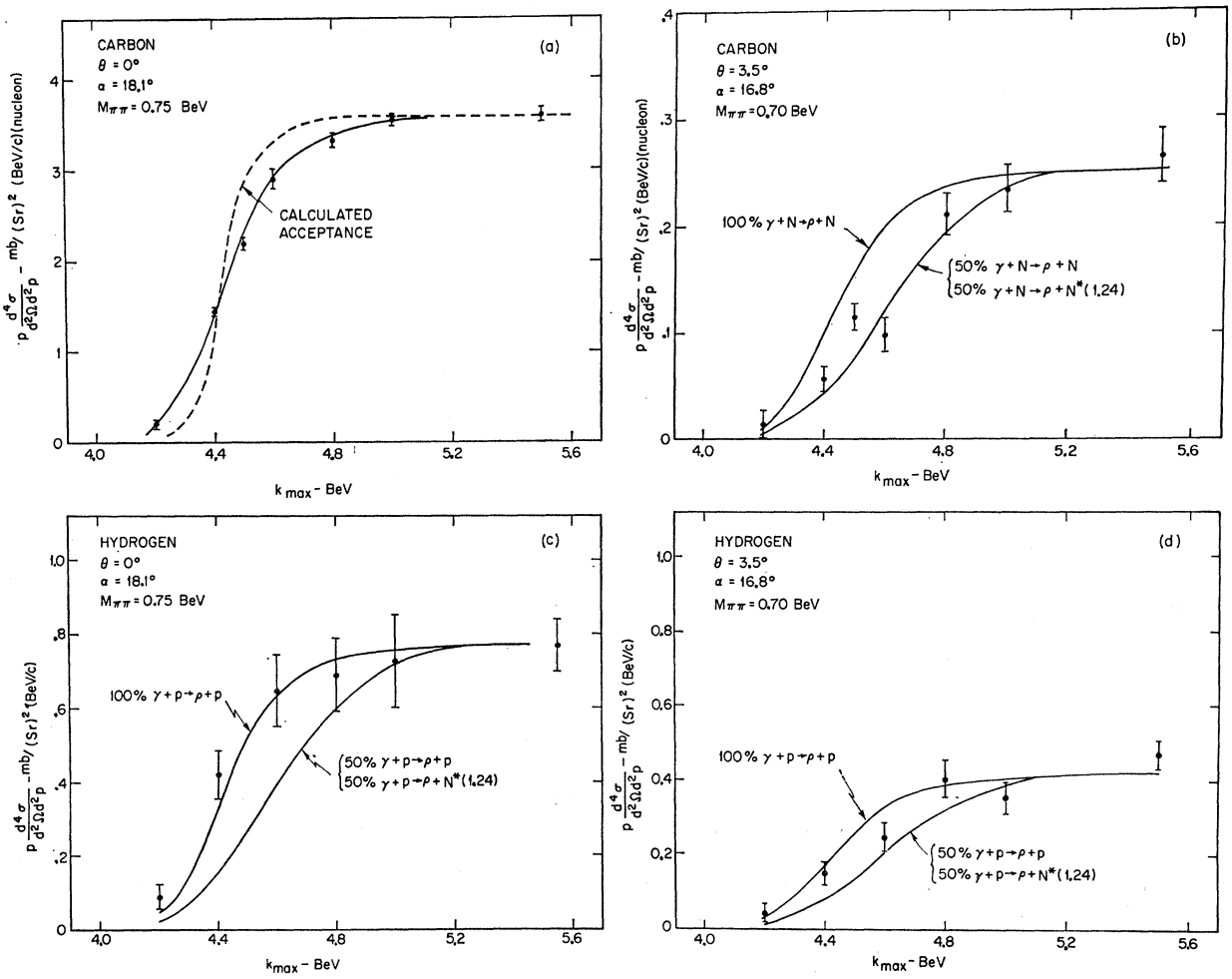

FIG. 8. Excitation curves for the production of two 2.2-BeV/c pions with $\alpha=18.2°$ and 16.8°. The abscissa k_{max} is the maximum photon-energy of the bremsstrahlung beam. Predicted yield curves normalized to the data with k_{max} between 5.0 and 5.5 BeV for mixtures of elastic ρ production and the inelastic process $\gamma+p\rightarrow\rho+N^*(1238)$ are also shown.

inelastic contribution is evidently large. A correction of $(50\pm20)\%$ has been applied to these data.

For the spectra obtained at the larger pion pair opening angle, the maximum γ-ray energy in the incoming beam (5.5 BeV) exceeds the observed ρ energy (2.5 BeV) considerably. The data in Figs. 9(a) and 9(b) were obtained with the maximum bremsstrahlung energy reduced to 3.0 BeV. The yield in the ρ^0 region is reduced by $(40\pm20)\%$ by this change. It is assumed that the additional rate at 5.5 BeV is due to inelastic contamination and the rate at 5.5 BeV has been appropriately corrected. For the carbon data, where we do not have the spectra corresponding to Fig. 9, we have subtracted an inelastic contribution per nucleon equal to that observed in hydrogen.

The formula required to convert the laboratory differential cross section for ρ production to the cross section expressed in terms of the invariant 4-momentum t is

$$\frac{d\sigma}{dt}=\frac{\pi}{kp_\rho}\frac{d\sigma}{d\Omega}\left[\frac{1-(\beta_{cm}E_p/p_p)\cos\theta_p}{1-\beta_{cm}}\right]. \quad (6)$$

Table I summarizes the measured differential cross sections and gives the correction which was made for inelastic contributions. These same data are shown plotted versus t in Fig. 10. The values of t have been averaged over the $\pm0.6°$ angular acceptance for ρ^0's. Also shown in this graph are the recent bubble-chamber measurements.[11–13]

V. DISCUSSION OF RESULTS

Three models have been suggested for understanding the photoproduction of neutral ρ mesons—the multiperipheral-diffraction model of Drell and Berman,[4] the one-pion exchange (OPE) model,[4] and the diffraction dissociation or its present-day equivalent, the vector-meson-dominance model.[14] The diagrams for these models are shown in Fig. 11. We shall briefly discuss each of the three models.

The cross section at small momentum transfer for the diffraction mechanism of Fig. 11(a) is[4]

$$\left[\frac{d\sigma}{dt}(s,t)\right]_{\gamma p\to\rho^0 p}=\left(\frac{p_\rho}{E_\rho}\right)\frac{(g_{\omega\pi\gamma}^2/4\pi)(g_{\rho\pi\omega}^2/4\pi)}{(48\Gamma_\rho/m_\rho)^2}\times\left[\frac{d\sigma}{dt}(s,t)\right]_{\pi p\to\pi\rho}. \quad (7)$$

Here $g_{\omega\pi\gamma}$ and $g_{\rho\pi\omega}$ are the coupling constants at the upper vertices in Fig. 11(a), and Γ_ρ is the $\rho^0\to2\pi$ decay width. According to this formula, $d\sigma/dt$ for ρ^0 photoproduction should vary with the c.m. energy s and the momentum transfer t in the same way as $d\sigma/dt$ for π-p elastic scattering. Experimentally, $d\sigma/dt$ for elastic π scattering is well described for small t by

$$[d\sigma/dt]_{\pi p\to\pi p}=(\sigma_{\pi p}/4\pi)^2e^{Bt}, \quad (8)$$

where $\sigma_{\pi p}$ is the total cross section for pions on protons[15] and $B=9.6\pm2.0$ BeV^{-2} for incident pions in the range 2–5 BeV.[16] If we use Eq. (8) for $(d\sigma/dt)_{\pi p\to\pi p}$, we obtain for the ratio of the 0° ρ^0 photoproduction cross sections from hydrogen at 2.5 and 4.4 BeV:

$$\left.\frac{d\sigma/dt(4.4\text{ BeV})}{d\sigma/dt(2.5\text{ BeV})}\right|_{\text{diffraction}}=0.84. \quad (9)$$

The expression for the cross section due to the OPE process of Fig. 11(b) is[4]

$$\frac{d\sigma}{dt}=\left(\frac{g_{\pi NN}^2}{4\pi}\right)\left(\frac{\Gamma_{\rho\pi\gamma}}{m_\rho}\right)\frac{|t|}{m_\rho^2}\frac{3p_\rho}{2k^2}\left[\frac{|t|+m_\rho^2}{|t|+m_\pi^2}\right]^2\frac{1}{M^2B}. \quad (10)$$

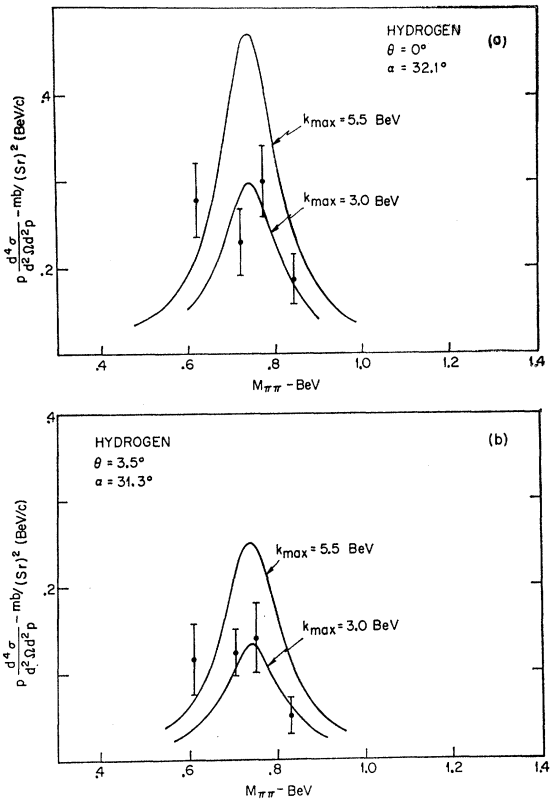

FIG. 9. Yields per equivalent quantum of pion pairs at the mass of the ρ with opening angles α of 32.1° and 31.3°. The upper curves were taken with a maximum bremsstrahlung energy of 5.5 BeV, the lower curves were for a maximum bremsstrahlung energy of 3.0 BeV. Only the data points for $k_{\max}=3$ BeV are shown. Much more data were available for $k_{\max}=5.5$ BeV.

[11] Cambridge Bubble Chamber Group, Phys. Rev. **146**, 994 (1966).
[12] Y. Eisenberg, E. E. Ronat, A. Brandstetter, A. Levy, and E. Gotsman, Phys. Letters **22**, 217 (1966).
[13] Aachen-Berlin-Bonn-Hamburg-Heidelberg-München Collaboration, Nuovo Cimento **41**, 270 (1966); DESY-Bericht 66/32 (unpublished); Nuovo Cimento **46**, 795 (1966); **48**, 262 (1967).
[14] M. Ross and L. Stodolsky, Phys. Rev. **149**, 1172 (1966).
[15] A. Citron, W. Galbraith, T. F. Kycia, B. A. Leontic, R. H. Phillips, and A. Rousset, Phys. Rev. Letters **13**, 205 (1964).
[16] M. L. Perl, L. W. Jones, and C. C. Ting, Phys. Rev. **132**, 1252 (1963).

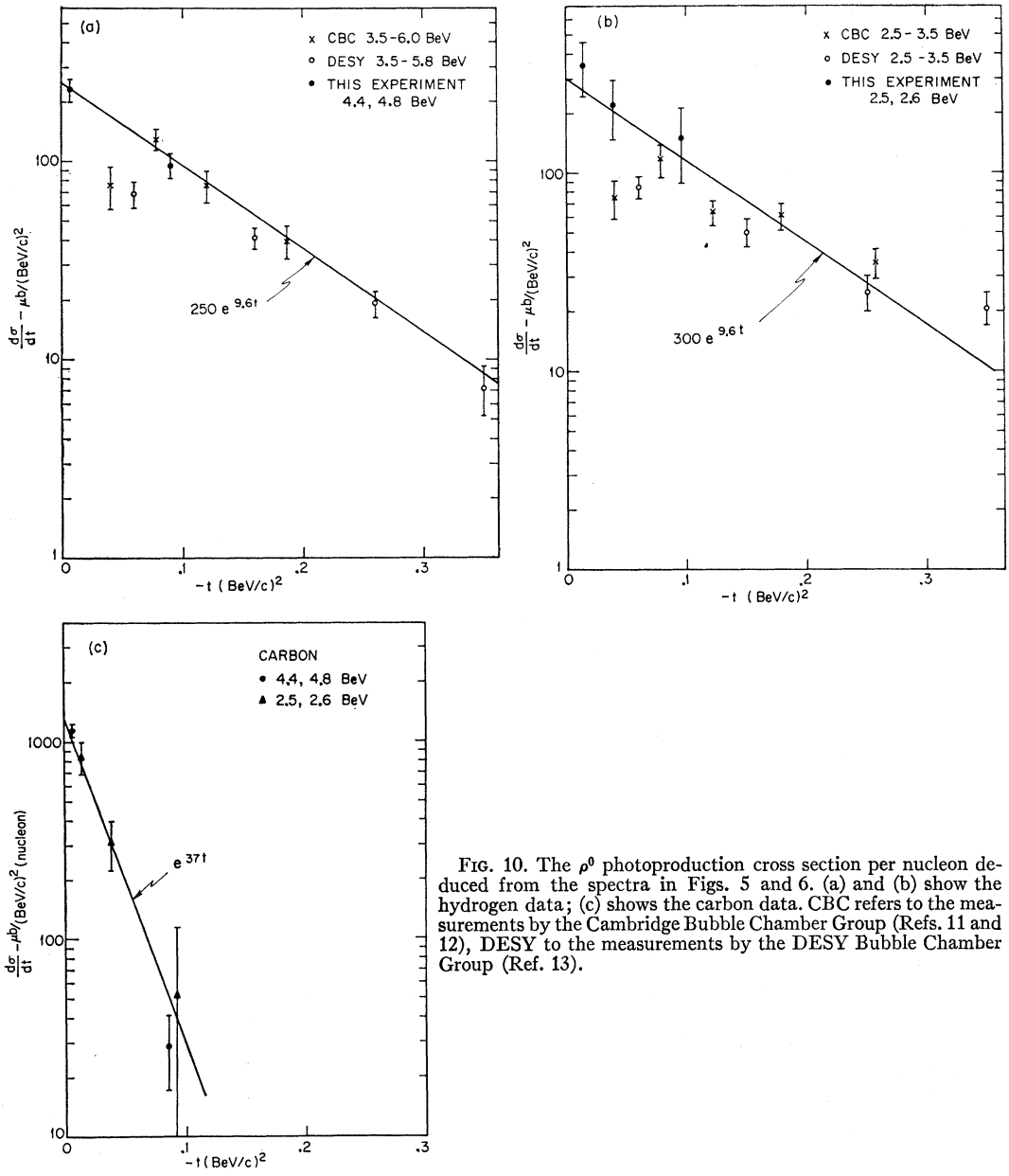

FIG. 10. The ρ^0 photoproduction cross section per nucleon deduced from the spectra in Figs. 5 and 6. (a) and (b) show the hydrogen data; (c) shows the carbon data. CBC refers to the measurements by the Cambridge Bubble Chamber Group (Refs. 11 and 12), DESY to the measurements by the DESY Bubble Chamber Group (Ref. 13).

Here $g_{\pi NN}$ is the coupling constant at the πN vertex, $\Gamma_{\rho\pi\gamma}$ is the partial decay width for $\rho^0 \rightarrow \pi^0+\gamma$, M is the proton mass, and B is a factor which is nearly unity for the conditions in this experiment. For production of a ρ^0 at 0°, $|t|$ is not zero but is equal to $|t_{\min}| \cong (m_\rho^2/2k)^2$. Thus at 0° the OPE cross section decreases as k^{-4}. After integrating Eq. (6) over the acceptance of the apparatus, we obtain an expected ratio

$$\left.\frac{d\sigma/dt(4.4\text{ BeV})}{d\sigma/dt(2.5\text{ BeV})}\right|_{\text{OPE}} = 0.21. \tag{11}$$

The experimental ratio is 0.66 ± 0.22. If we treat the observed cross sections as an incoherent combination of OPE and diffraction production, we obtain for 4.4 BeV the partial cross sections

$$\begin{aligned} d\sigma/dt(\text{OPE}) &= 21\pm97\ \mu\text{b/BeV}^2, \\ d\sigma/dt(\text{diff}) &= 210\pm52\ \mu\text{b/BeV}^2. \end{aligned} \tag{12}$$

This shows that for hydrogen the production is dominated by the diffraction mechanism. The value of $\Gamma_{\rho\pi\gamma}$ deduced from this OPE cross section is 2 ± 10 MeV. Other experiments place an upper limit of 0.6 MeV on $\Gamma_{\rho\pi\gamma}$.[17] The magnitude of the observed diffraction cross section is correctly predicted by Eq. (7) if we use

[17] G. Fidecaro, M. Fidecaro, J. A. Poirier, and P. Schiavon, Phys. Letters 23, 163 (1966).

$g_{\omega\pi\gamma}^2/4\pi=0.03$ and $g_{\rho\pi\omega}^2/4\pi=12$. This value of $g_{\omega\pi\gamma}$ corresponds to a partial width for the decay of the ω, $\Gamma_{\omega\pi\gamma}$, of 1 MeV; the measured width for decay into neutrals is 1.16 MeV.[18] This value of $g_{\rho\pi\omega}$ is the same as the value deduced assuming ω decay is dominated by $\omega\rightarrow\rho+\pi\rightarrow 3\pi$.[19]

For carbon, the relative contribution of inelastic processes should be less since the diffraction mechanism should behave coherently and produce a very large cross section in the forward direction. Also, for carbon the angular distribution should be much more sharply peaked forward for the diffraction mechanism. That this is true is shown by the data in Figs. 6 and 10(c). For carbon, the variation of the 0° cross section with energy is consistent with a pure diffraction mechanism The momentum-transfer dependence of the cross section is fit with $B=37$ BeV^2; this value for B agrees with what one expects on the basis of an optical model.

In addition to the data from this experiment, Figs. 10(a) and 10(b) show the data from the measurements of the Cambridge Bubble Chamber Group[11] and the DESY Bubble Chamber Group.[13] The DESY data were presented in the original publication in terms of $d\sigma/dt$ versus $-t$ averaged over a range of incident γ-ray energies; the Cambridge data have been converted from $d\sigma/d\Omega^*$ versus $\cos\theta^*$, where θ^* is the c.m. production angle of the ρ to $d\sigma/dt$ versus t by using the mean value of the incident γ energy reported for each interval. The Cambridge data were taken from the paper of Eisenberg *et al.*,[12] in which the θ^* intervals into which the events are grouped are smaller than in the earlier report of the same data by the Cambridge Bubble Chamber Group. In the $3.5<k<6.0$ BeV interval, the bubble-chamber data at $-t>0.06$ BeV^2 agree rather well with the data of this experiment if both are fitted to the $e^{9.6t}$ dependence suggested by the diffraction model. At small t values, the bubble-chamber data fall below the exponential. It is observed by Eisenberg *et al.* that the lowest t point suffers from experimental biases due to the detection of short proton recoil tracks. An attempt to correct for this effect in the report of the Cambridge Bubble Chamber Group[11] leads to a cross section extrapolated to 0° of 0.60 ± 0.15 mb/sr, less than $\frac{1}{2}$ that observed in this experiment; the fit of Eisenberg *et al.*[12] to the same data, ignoring the lowest t point, gives a value of $d\sigma/dt$ at 0° three standard deviations above that including all the data.

The data from the DESY chamber fit a t dependence $e^{7.7t}$ rather well at higher incoming γ-ray energies.[13] π-p scattering in the range $0<-t<0.8$ (BeV/c)^2 is, however, rather poorly described by such a t dependence; a term in t^2 is required to fit the data well.[12] The initial slope is then 9.6 (BeV/c)$^{-2}$ rather than 7.7 (BeV/c)$^{-2}$. The results of our experiment for ρ^0 production near 0° are consistent with those of the bubble chambers and a 9.6 (BeV/c)$^{-2}$ slope for small t except for the bubble-chamber points at their lowest t value. At 4.4 BeV, our 0° cross section with this shape corresponds to a total cross section of 22 ± 5 μb, a value considerably higher than that obtained in the bubble-chamber experiments.

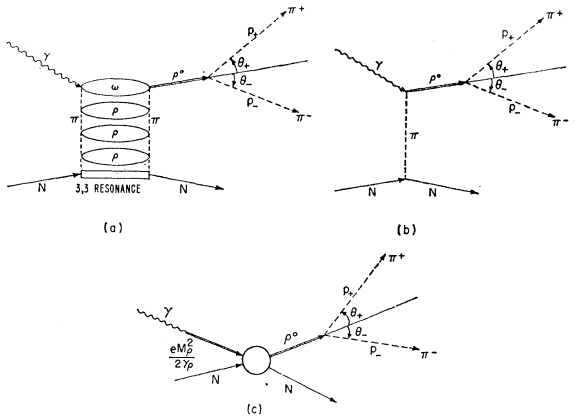

FIG. 11. Diagrams of possible ρ^0 photoproduction processes. (a) is for diffractionlike production in the multiperipheral model; (b) is for single-pion exchange; (c) is for the diffraction-dissociation or vector-meson-dominance model.

In their treatment of the diffraction dissociation model, Ross and Stodolsky[14] postulate a certain amplitude for the photon to change into a ρ meson and then calculate the photoproduction cross section using this model. They find that they can understand the main features of ρ photoproduction. Since they give a rather extensive treatment of this problem using the data that we are reporting here, we shall not repeat their conclusions.

In addition to predicting the ρ photoproduction cross section, Ross and Stodolsky also predict that the mass spectrum for the photoproduction will be described by the function

$$\left(\frac{m_\rho}{m}\right)^{4}\frac{1}{\pi}\frac{\frac{1}{2}\Gamma}{(m-m_\rho)^2+(\frac{1}{2}\Gamma)^2}, \tag{13}$$

rather than the conventional BW function. This form of the mass spectrum predicts that the peak will occur at a lower mass than that corresponding to the ρ. This could explain the lower ρ mass found in this experiment.

It has become popular to treat the ρ-photon coupling in terms of what is called the vector-meson-dominance model.[20] In this model, it is assumed that the photon

[18] A. H. Rosenfeld, A. Barbaro-Galtieri, W. J. Podolsky, L. R. Price, P. Soding, C. G. Wohl, M. Ross, and W. J. Willis, Rev. Mod. Phys. **39**, 1 (1967).

[19] M. Gell-Mann, D. Sharp, and W. G. Wagner, Phys. Rev. Letters 8, 261 (1962).

[20] Some of the other papers containing material relevant to the vector-dominance model are the following: (a) J. J. Sakurai, Ann. Phys. (N.Y.) **11**, 1 (1960); (b) M. Gell-Mann and F. Zachariasen, Phys. Rev. **124**, 953 (1961); (c) M. Gell-Mann, *ibid.* **125**, 1067 (1962); (d) R. F. Dashen and D. H. Sharp, *ibid.* **133**, B1585 (1964); (e) D. S. Beder, *ibid.* **149**, 1203 (1966); (f) P. C. O. Freund, Nuovo Cimento **44**, A411 (1966); (g) H. Joos, Phys. Letters **256**, 103 (1967); (h) H. Joos, DESY-Bericht 67/13, 1967 (unpublished); (i) N. M. Kroll, T. D. Lee, and B. Zumino, Phys. Rev. **157**, 1376 (1967).

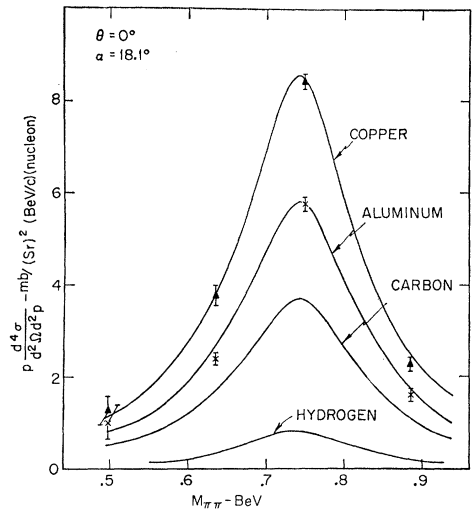

FIG. 12. Pion pair production per nucleon for copper, aluminum, carbon, and hydrogen targets. The opening angle α between the pair is 18.2°; the resultant momentum of the pair lies along the direction of the incoming γ-ray beam.

interacts with the hadrons only through the three vector mesons: the ρ, the φ, and the ω. Thus one can relate all photoproduction amplitudes to strong-interaction processes involving the vector mesons. This model relates ρ photoproduction from hydrogen to ρ-proton elastic scattering. The precise form of the relation is

$$\frac{d\sigma}{dt}(\gamma+p\rightarrow\rho^0+p)=\tfrac{1}{4}\alpha\left(\frac{4\pi}{\gamma_\rho{}^2}\right)\frac{d\sigma}{dt}(\rho^0+p\rightarrow\rho^0+p). \quad (14)$$

The γ-ray–vector-meson coupling constant γ_ρ can be derived from a study of the leptonic decay of the ρ, the pion form factor, and the widths for the decays of the vector mesons into $\pi^0+\gamma$. This model seems to be quite successful, although a great deal more data are needed to evaluate it properly.

VI. *A* DEPENDENCE OF ρ^0 PRODUCTION AT 0°

Further evidence for dominance of the diffraction mechanism in ρ^0 photoproduction comes from the variation of the 0° cross section with the atomic number of the target nucleus. Only for a process in which no quantum numbers are exchanged with the target particle can the production cross section per nucleon increase with atomic number. OPE, for example, in which isospin is exchanged with the target protons, cannot behave coherently. In Fig. 12 are shown, normalized to the same number of nucleons, the momentum spectra observed in hydrogen, carbon, aluminum, and copper for $\theta=0°$ and a pion opening angle of 18.2°. Table II and Fig. 13 give the corresponding 0° ρ^0 production cross sections per nucleon. Corrections have been applied to the data for absorption in the target of the incoming γ rays and outgoing pions. Each correction is less than 10%, except for the γ-ray correction in copper which is 22%.

A detailed understanding of Fig. 13 requires a model of nuclear-absorption effects. A comparison with the A dependence of π-nucleus scattering, which is also shown in Fig. 13, shows clearly the close relation between the processes. The A dependence also precludes an appreciable contribution to the hydrogen cross section from processes involving an exchange of quantum numbers. Since for photoproduction the invariant momentum transfer t is not zero at 0°, some decrease with A relative to elastic scattering is expected in addition to that from absorption corrections.

In a study of ρ^0 production, Ross and Stodolsky[14] have used the diffraction dissociation model, in which production of particles having the same quantum numbers as the photon occurs because of different diffraction scattering on the target nucleus. In this model the ρ^0-N interaction is viewed as the "source" of the photoproduced ρ's. Using an optical-model calculation for the ρ-nucleus scattering, they fit these data with $\sigma(\rho\text{-}p)=50\pm5$ mb (statistical error only).

Drell and Trefil[21] have analyzed these same data on an optical-model basis which treats the ρ-nucleon interaction as a correction to the outgoing ρ^0 flux. When it is applied only to the complex nuclei cross sections, their calculation requires $66\leq\sigma_t(\rho\text{-}p)\leq94$ mb. Since the two methods for analysis of the ρ^0 cross sections are very similar, the differences in the values of $\sigma_t(\rho\text{-}p)$ obtained may be due to the choice of different optical-model parameters and the inclusion, in one case, of the hydrogen data. [*Note added in proof.* In their calculation of the ρ-nucleon total cross section, Drell and Trefil assumed that the momentum transfer for the 0°

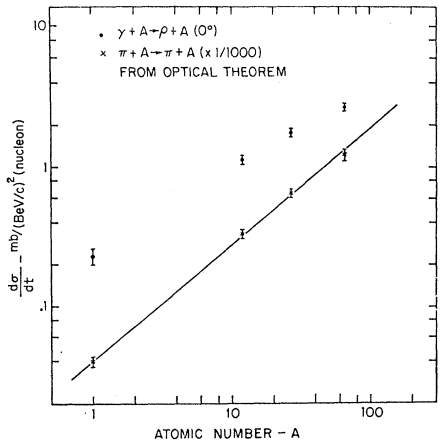

FIG. 13. The 0° ρ^0 production cross sections per nucleon deduced from the spectra in Fig. 12. For comparison, the corresponding 0° pion-nucleus elastic scattering cross sections per nucleon are also shown. The pion-nucleus cross sections were calculated from the measured total cross sections by using the optical theorem.

[21] S. D. Drell and J. S. Trefil, Phys. Rev. Letters **16**, 552 (1966); **16**, 832 (1966).

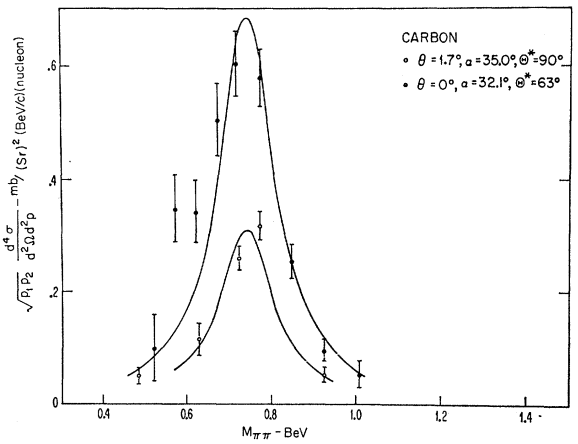

FIG. 14. Pair mass spectrum with unequal momenta chosen to correspond to an angle of 63° between the direction of the ρ^0 and one of the decay pion as viewed in the ρ^0 rest system.

cross sections reported in our earlier publication was the minimum transfer corresponding to exactly 0° production. The actual cross sections were, however, the average cross sections determined by the small but finite solid-angle acceptance of the apparatus. Thus, in making their analysis, Drell and Trefil did not correct the data for the finite angular acceptance of the apparatus. Because of the steep momentum transfer dependence of the cross sections, this correction is quite significant. If one corrects the measured cross sections for the depression due to the momentum transfer dependences and uses the corrected cross sections to repeat the Drell-Trefil analysis one obtains a ρ-nucleon cross section consistent with 30 mb.]

VII. ϱ DECAY DISTRIBUTION AND ϱ POLARIZATION

Data were also taken to study the production of ρ's which decay asymmetrically with respect to their line of flight. At $\alpha=34°$ (2.3-BeV ρ^0), the angles and momenta of the spectrometer arms were set to detect decay pions from a ρ produced forward but decaying at 63° with respect to its line of flight. The laboratory angles of the pions were, for this case, 9.4° and 24.8°; the corresponding momenta for $M_{\pi\pi}=750$ MeV were 1.77 and 0.73 BeV/c. Because the two magnet apertures are equal distances above and below the horizontal plane, the plane of the detected pions does not contain the incoming γ-ray direction except when the pions make equal angles with the γ ray. For the asymmetric decay described above, the angle of the ρ^0 with respect to the γ ray is 1.7°.

The spectra of asymmetric pairs were taken with both possible sign configurations for the pair. Within 12%, the rates at the points near the ρ peak were equal. This is in striking contrast to the observation for ρ's produced in strong interactions of a large forward-background asymmetry of ρ decay.[22] Together with the lower mass and greater width of the ρ observed in this experiment, it supports the view that a strong s-wave π-π production is excited in the strong-interaction[23] experiments. Such a state would be expected to be suppressed in a photoproduction process with small momentum transfer.

In Fig. 14 is shown the pion-pair mass spectrum obtained. Also shown is the fit to the spectrum of symmetrically produced pairs of the same total energy from Fig. 6(c). The expected slight decrease in yield due to the larger ρ production angle in the asymmetric case is taken into account using the e^{37t} fit to the data of Fig. 10(c). The relative number of decays at 63° and 90° in the ρ^0 rest system is

$$\frac{\rho^0\rightarrow 2\pi(63°)}{\rho^0\rightarrow 2\pi(90°)}=0.81\pm0.08. \qquad (15)$$

For complete transverse polarization of the ρ's, as must occur in a coherent non-spin-flip process, the expected ratio is 0.78. From these data we conclude that the ρ's produced from carbon are polarized. The reduction of the observed pair rates to ρ^0 production cross sections in Sec. IV assumed polarization in hydrogen as well as carbon.

VIII. PRODUCTION OF OTHER RESONANCES

Although the mass spectra shown in Figs. 5 and 6 individually show features which suggest other resonant structure than the ρ, over-all they do not give clear evidence for any other resonance produced by a simple process. A more detailed experimental search of this mass region is obviously desirable.

From these spectra, lower limits can be placed on the production of other known two-particle resonant states. The f^0 ($m=1250$ MeV, $\Gamma=120$ MeV, 67% decay to $\pi^+\pi^-$) contribution to the 6.5° mass spectrum in carbon is less than 5% of that of the ρ^0 at the ρ^0 peak [Fig. 5(e)]. Since an f^0 has spin 2, if it is produced by a process

TABLE II. Cross sections per nucleon for photoproduction of ρ's from various nuclei. For these measurements the energy of the ρ was 4.4 BeV. These 0° cross sections have not been corrected for the finite angular acceptance of the apparatus.

Target	$(1/A)d\sigma/dt$ [mb/(BeV/c)²]
Hydrogen	0.23±0.03
Carbon	1.14±0.08
Aluminum	1.76±0.11
Copper	2.69±0.16

[22] I. Derado, V. P. Kenney, J. A. Poirier, and W. D. Shephard, Phys. Rev. Letters 14, 872 (1965).
[23] L. Durand, III, and Y. T. Chiu, Phys. Rev. Letters 14, 329 (1965).

which preserves the incoming γ-ray polarization it cannot contribute to the 0° and 3.5° spectra; both the 0° and 3.5° spectra involve pions which are emitted at 90° with respect to the γ-ray direction as seen in the f^0 rest system. If we allow for the difference in decay widths, detection efficiencies, and c.m. energies, the corresponding f^0 production cross section from carbon is less than 0.5% of the ρ^0 cross section at the same angle; that is, $d\sigma/dt$ (f^0) is less than 0.8 μb/(BeV/c)^2. Since the 4-momentum transfer for f^0 production at 6.5° is $t=-0.26$ (BeV/c)^2, one would expect primarily inelastic, hydrogenlike, production of the f^0. Comparing

$$(1/A)d\sigma/dt(\gamma+p\rightarrow f^0+\text{anything})$$

at $t=-0.26$ (BeV/c)^2 with the observed hydrogen cross section at the same t value [$d\sigma/dt(\gamma+p\rightarrow p+\rho)=20$ μb/(BeV/c)^2]. we conclude that for a diffraction process, f^0 production in hydrogen is less than 4% of the ρ^0 production.

The decay of neutral K mesons produced in the target would also be observed. Since the mass of the K_1 is well defined, it would appear as a peak at $M_{\pi\pi}=498$ MeV broadened only by the mass resolution of the system. The distribution in space of K_1 decays does not broaden the mass resolution since to a good approximation the invariant-mass resolution is independent of the location in the horizontal plane of the two-pion vertex. At the small opening angle, a K_1 production cross section $d\sigma/d\Omega$ equal to the ρ cross section would produce a peak in the mass spectrum 60 MeV wide and two times the maximum ρ rate observed; at the larger opening angle, the peak would be 40 MeV wide and enhanced relative to the ρ by a factor of 3.

Examination of all of the spectra puts an upper limit of 50 μb/sr on the cross section for producing a K_1 via any two-body processes, $\gamma+p\rightarrow K^0+Y^*$, involving Y^* excitation energies ≤ 2 BeV. For three-body processes we can give only a limit to $d\sigma/d\Omega dp$, the cross section per equivalent quantum, for producing a K_1 in the momentum range dp and in the solid angle $d\Omega$. The upper limit for this cross section is ~ 300 μb/sr (BeV/c).

IX. SUMMARY

We conclude that in the 2–5 BeV range of incoming γ rays the process $\gamma+p\rightarrow p+\pi^+ +\pi^-$ occurs an appreciable fraction of time in the two-body channel $\gamma+p\rightarrow\rho^0+p$. From the dependence of the pion pair yield in the ρ^0 mass range on incoming γ-ray energy, momentum transfer, and atomic number of the target nucleus, we conclude that the reaction $\gamma+p\rightarrow\rho^0+p$ proceeds predominantly via a diffractionlike process involving no exchange of quantum numbers with the target. In contrast to ρ^0 production by strongly interacting particles, we find no front-back asymmetry in the decay process and a decay width $\Gamma=160\pm 10$ MeV considerably larger than the generally accepted value of 120 MeV.

In the analysis reported here, we have chosen to use a BW curve rather than the modified curve of Ross and Stodolsky to analyze the data. If we had used the modified curve, we would have obtained a higher mass of the ρ which is in better agreement with the accepted value. It is clear from the spectra that there is a large low-mass background which is at present not understood. Until one knows more about this background, it is difficult to analyze unambiguously the data. In the light of this background and the method we have used to analyze the data, the quoted cross sections should be considered as upper limits.

ACKNOWLEDGMENTS

We wish to acknowledge the support given to us by the staff of the Harvard Cyclotron Laboratory and the staff of the Cambridge Electron Accelerator. We wish to express thanks to Joseph McSherry and Bert Farmer for help with the hydrogen target, to Carl Friedberg for the i.d. system, and to Miss Nancy Hicks, Bent Huld, and Lawrence Litt, for aid in taking data. We are indebted to Professor S. Berman, Professor S. Drell, Professor M. Ross and Professor L. Stodolsky for illuminating discussions of the theory. The speed with which the apparatus was set up is a tribute to Arthur Sansone and William Sansone.